Journal of Power Sources 219 (2012) 9–15

Contents lists available at SciVerse ScienceDirect

Journal of Power Sources

journal homepage: www.elsevier.com/locate/jpowsour

Thin ZnO nanocrystalline films for efficient quasi-solid state electrolyte quantum dot sensitized solar cells

Dimitrios Karageorgopoulos [a,b], Elias Stathatos [a,*], Evangelos Vitoratos [b]

[a] Department of Electrical Engineering, Technological-Educational Institute of Patras, GR-263 34 Patras, Greece
[b] Department of Physics, University of Patras, GR-26500 Patras, Greece

HIGHLIGHTS

- Novel and facile method for thin ZnO nanocomposite films.
- Different ZnO film morphologies with solution components variation.
- CdSe quantum dots were assembled onto ZnO films via wet method.
- 4.5% maximum photo-electrochemical cell performance of CdSe sensitized ZnO films.

GRAPHICAL ABSTRACT

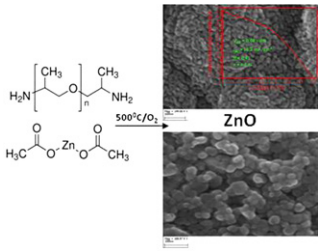

ARTICLE INFO

Article history:
Received 8 June 2012
Received in revised form
2 July 2012
Accepted 13 July 2012
Available online 20 July 2012

Keywords:
ZnO
Thin films
Quantum dot sensitized solar cells
Quasi-solid state electrolyte

ABSTRACT

Thin transparent ZnO nanocrystalline films are prepared through a novel facile method based on an amino double edged polypropylene oligomer and zinc precursor. While amines were reacted with acetate groups of zinc acetate starting material, the polypropylene oligomers acted as template for the oxide formation. Different structural properties of the ZnO films were achieved varying the quantity of the oligomer in the starting solution. Spherical aggregated or monodispersed particles were formed with average sizes ranging from 10 to 30 nm. The films were employed in the construction of quantum dot sensitized solar cells using both CdS and CdSe. For first time a quasi solid state electrolyte was applied succeeding a maximum overall efficiency of 4.5% in the case of aggregated particles which could probably act as scattering centers. The quasi solid state electrolyte was a hybrid organic–inorganic material with SiO_2 edged groups while no water was used in any step of preparation of the host electrolyte for a polysulfide redox couple.

1. Introduction

Utilization of renewable energies is of major importance because of the increase in fossil energy costs and future shortages. Taking into account the present status in photovoltaic technology some progress has to be made in cost/Watt and applicability. For this reason developments on potentially cheaper solar cells have made based on mesoporous wide band gap metal oxides inorganic semiconductors [1–3]. Dye sensitized solar cells (DSSCs) for almost twenty years have proved themselves as low cost alternatives in conventional technology based on silicon [4,5]. The almost 12% efficiency of these cells is mainly due to the unique properties of the nanostructured metal oxides n-type semiconductors typically TiO_2 [6]. ZnO is also a wide band gap semiconductor with energy band structure and physical properties similar with TiO_2 [7]. However, it has higher electronic mobility (155 $cm^2\ v^{-1}\ s^{-1}$ vs to 10^{-5} $cm^2\ v^{-1}\ s^{-1}$ of TiO_2) favorable for electron transport, it is easily crystallized and anisotropically grow in a variety of morphologies [8,9].

One of the main factors that limit the efficiency of the DSSCs and increase their cost is the dye used for inorganic semiconductors sensitization in the visible and near IR region of the solar spectrum [10]. Ruthenium-based dyes are usually costly while their extinction

* Corresponding author. Tel.: +30 2610 369242; fax: +30 2610 369193.
E-mail address: estathatos@teipat.gr (E. Stathatos).

0378-7753/$ – see front matter © 2012 Elsevier B.V. All rights reserved.
http://dx.doi.org/10.1016/j.jpowsour.2012.07.034

coefficients and absorption spectra could not effectively cover the requirements for high efficient solar cells [11]. Recent developments in the field showed that semiconductor quantum dots (QDs) could effectively sensitize wide band gap metal oxides instead of organic dyes [12]. Semiconductor QDs in the form of very small crystals could be very stable while present the advantage to match solar spectrum better because their absorption spectrum can be tailored by size quantization [13,14]. Moreover, the possibility of generation of multiple electron–hole pairs from one photon could lead to very high theoretical efficiencies exceeding 66% [15]. To date a wide range of QDs are used to the fabrication of QD sensitized solar cells (QDSSCs) in combination with wide band gap inorganic semiconductors (TiO_2, ZnO) and a redox electrolyte [16,17]. Among QDs, CdSe [18], CdS [19], CdTe [20], PbS [21], PbSe [22] and some combinations of them are more often referred to the construction of efficient QDSSCs while a maximum 4.2% efficiency is recorded for a TiO_2/CdS/CdSe composite system [23]. The TiO_2 or ZnO modification with QDs can be achieved by in situ growth of QDs using chemical bath deposition (CBD) [24], successive ionic layer adsorption and reaction (SILAR) [25] or deposition of presynthesized colloid QDs in direct (DA) [26] or by linker assisted adsorption (LA) [27].

There is, however, very little work done with solid-state Quantum Dot Sensitized Solar Cells prepared from colloids [28,29], while there are no references for quasi-solid state electrolytes based on nanocomposite materials. The majority of literature is referred in liquid based mainly aqueous electrolytes although further investigations should be presented on solid/quasi-solid electrolytes as they exhibit practical benefits on the stability and longevity of the cells. In present work a novel facile method for the formation of ZnO nanostructured films is described. According to this method zinc acetate readily react with low molecular weight poly(propylene glycol) ended by amine groups at both edges. Co-sensitization of the zinc oxide films with CdS/CdSe QDs are discussed while a quasi solid state electrolyte employing polysulfide (S^{2-}/S_x^{2-}) redox couple is used for first time in the QDSSC completion.

2. Experimental

2.1. Materials

Zinc acetate (Znacac, 98%, Aldrich), poly(propylene glycol) bis(2-aminopropyl) ether ($CH_3CH(NH_2)CH_2[OCH_2CH(CH_3)]_nNH_2$ average $M_n \approx 230$, BAPPG, Aldrich), Cadmium nitrate tetrahydrate (98%, Aldrich), Selenium powder (99,999%, Aldrich), sulfur powder (99,5%, Aldrich), Nitrilotriacetic acid trisodium salt ($C_6H_6NO_6Na_3$, Na_3NTAA, 98%, Sigma), Sodium sulfide (98%, Aldrich), Sodium sulfite (98%, Aldrich), 3-isocyanatopropyltriethoxysilane ($(C_2H_5O)_3Si(CH_2)_3NCO$, 95%, Aldrich), hydrogen hexachloroplatinate(IV) hydrate (H_2PtCl_6, 98%, Aldrich), Methanol (MeOH, pro-analysis, Merck), isopropanol (*i*-prOH, pro-analysis, Merck). All chemicals were of analytical grade and used without any further purification. SnO_2:F transparent conductive glasses (FTO, TEC15) 15 Ω square^{-1} were purchased from Hartford Glass Co., USA. The glasses prior use as substrates for ZnO films and QDs deposition were carefully cleaned with detergent and washed out with distilled water and isopropanol.

2.2. Preparation of ZnO films

First, 0.183 g of Zinc acetate were dissolved in 6 ml of *i*-prOH. Then, poly(propylene glycol) bis(2-aminopropyl) ether oligomer was added under vigorous steering in a molar ratio ranging from [BAPPG]:[Znacac] = 0.5–6 while Znacac content was always kept constant. The mixture was heated up to 80 °C in a closed bottle for 2 h and then it was naturally cooled down at room temperature. Films on FTO glasses were formed with dip-coating from above solutions. The withdrawal rate was 2 cm s^{-1}. After each FTO conductive glass was dipped into the sol and taken out, the coated composite material with ~2 cm^2 (2 cm × 1 cm) area was obtained by removing the adhesive tape which was used as a mask cut. The films were finally calcined up to 500 °C for 45 min total time. The furnace temperature was incremented at a ramp rate of 15 °C min^{-1} to 500 °C; this temperature was held for 15 min, then the coated FTO conductive glass was cooled to room temperature.

2.3. Preparation of ZnO/CdS/CdSe composite films

Successive ionic layer adsorption and reaction (SILAR) method was used to assemble CdS QDs onto ZnO films. According to this method each ZnO film was successively immersed into two different solutions for approximately 10 min, first in 0.1 M aqueous $Cd(NO_3)_2$ and then to 0.1 M aqueous Na_2S solution. Before each immersion, the films were rinsed with double distilled water and dried in a preheated oven at 100 °C. This constitutes one SILAR cycle. CdSe QDs onto ZnO/CdS films were formed by chemical bath deposition method (CBD). Before the application of CBD Na_2SeSO_3 salt synthesis was necessary as Se ions source. Na_2SeSO_3 aqueous solution is prepared by refluxing Se powder (0.1 M) in an aqueous solution of Na_2SO_3 (0.2 M) at 80 °C for 6 h until full dissolution of Se in Na_2SO_3 solution. For the CBD of the CdSe QDs, 10 ml of 0.2 M Na_3NTAA were added to 10 ml of 0.1 M $Cd(NO_3)_2$ followed by 10 ml of the as-prepared Na_2SeSO_3 aqueous solution [30]. An FTO glass covered with ZnO/CdS film was placed into the above solution and kept for several hours until the color of the film was turned into red. It was found that the procedure could be accelerated if it was carried out under artificial solar light. The films were thoroughly rinsed with distilled water to remove any residual material and dried in a preheated oven at 100 °C. In all samples ZnS capping was chosen to cover CdSe QDs for passivation [31]. The films were successively dipped in 0.1 M Zinc acetate and 0.1 M Na_2S aqueous solutions for 1 min for each dipping.

2.4. Film characterization

The crystal phase and grain size calculation for all prepared films of ZnO were determined by X-ray diffraction (XRD) using a Bruker

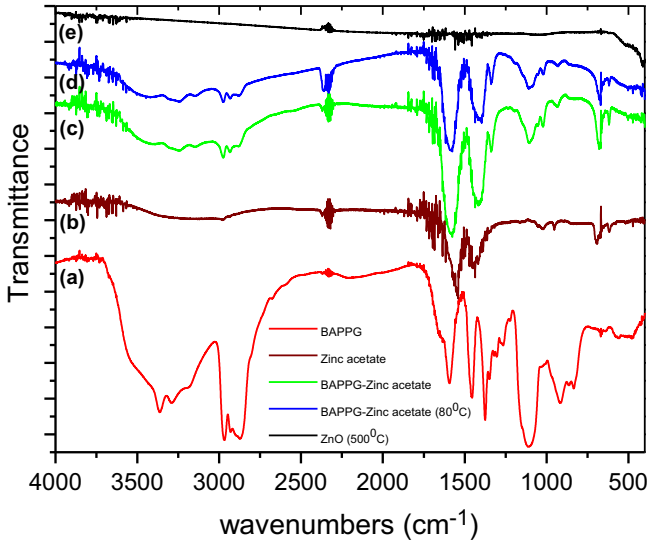

Fig. 1. FTIR spectra of (a) pure BAPPG, (b) Znacac and composite Zn-acac/BAPPG film after solvent evaporation (c) at room temperature or (d) at 80 °C. Calcined films at 500 °C are presented as (e).

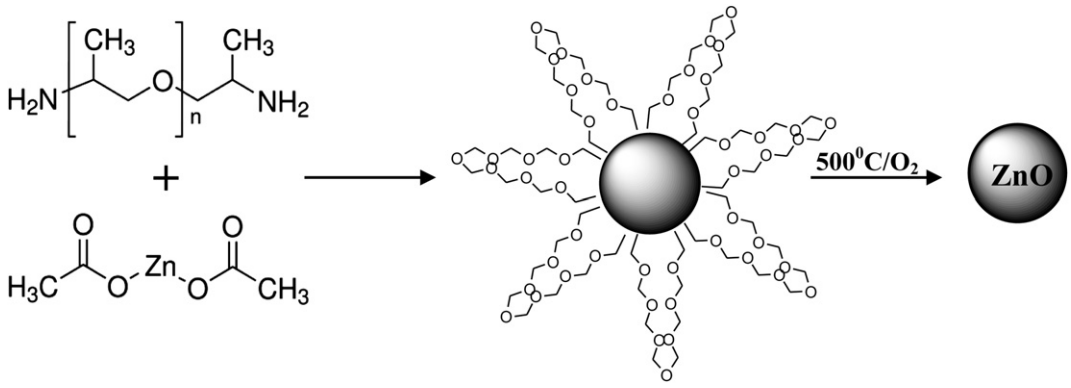

Scheme 1. Reaction mechanism for ZnO nanocomposite films formation.

D8 Advance diffractometer with CuKa ($\lambda = 1.5406$Å) radiation and Bragg-Brentano geometry. Film morphology and film thickness were characterized by Scanning Electron Microscopy (FE-SEM, Zeiss Leo Supra 35VP). Residual organic composition of the films and Zn–O bond formation were detected from FT-IR spectra which were monitored with a Jasco 4100 spectrophotometer while the films were prepared on silicon wafers avoiding the absorbance of the glass substrates in the infra red region. UV–Vis spectra of the ZnO and CdS/CdSe/ZnO composite films were obtained using a UV–Vis spectrophotometer (Hitachi, U-2900).

2.5. Preparation of quasi-solid state electrolyte for QDSSCs

In the construction of the solar cells a quasi-solid state electrolyte was used. This was chosen as a promising approach to QDSSC technology as it combines the high ionic conductivity of liquids while it reduces the risk of leaks and minimizes sealing problems in the cells. For the gel electrolyte applied to the QDSSCs, we used a hybrid organic–inorganic material ICS-PPG230 which was prepared according to a procedure described in previous publications and it successfully proved itself in long term stability and durability to the application of Dye sensitized solar cells [32–34]. Briefly, poly(propylene glycol)bis(2-aminopropyl ether) of molecular weight 230 and 3-isocyanatopropyltriethoxysilane (ICS; molar ratio ICS/diamine = 2) react in a vessel (acylation reaction), producing urea connecting groups between the polymer units and the inorganic part. The gel electrolyte was synthesized by the following procedure. 0.7 g of the functionalized alkoxide precursor ICS-PPG230 were dissolved in 2.4 g of MeOH under vigorous stirring. Then, 0.25 M S and 1 M Na_2S added to the previous sol and it was used as redox couple. Na_2S works as a hole scavenger (oxidized into S_2^{2-}) to prevent photocorrosion of CdSe [35]. After 2 h stirring, one drop of the obtained sol was placed on the top of the ZnO electrode modified with CdS/CdSe QDs and a slightly platinized SnO_2:F counter electrode was pushed by hand on the top. The platinized FTO glass was made by exposing it to a H_2PtCl_4 solution (5mg/1 ml of EtOH) followed by heating at 450 °C for 10 min. The two electrodes tightly stuck together by Si–O–Si bonds developed by the presence of ICS-PPG230 and ambient humidity.

2.6. Electrical characterization of the QDSSCs

For the *J–V* curves, the samples were illuminated with Xe light using a Solar Light Co. solar simulator (model XPS 400) equipped with AM 0 and AM 1.5 direct Air Mass filters to simulate solar radiation at the surface of the earth. The light intensity was kept constant at 1000 W m^{-2} measured with a CMP 3 Kipp & Zonen pyranometer. Finally, the *J–V* curves were recorded by connecting the cells to a Keithley Source Meter (model 2601) which was controlled by Keithley computer software (LabTracer). The cell active area for these measurements was 0.24 cm^2 using a mask while back reflectors were not used in the measurements. For each different sample, we have made three cells which were tested under the same conditions in order to avoid any misleading estimation of their efficiency. Cell performance parameters, including short-circuit current density (J_{SC}), open circuit voltage (V_{OC}), maximum power (P_{max}), fill factor (*ff*) and overall cell conversion efficiency, were measured and calculated from each *J–V* characteristic curve.

3. Results and discussion

In present work a facile procedure for the preparation of ZnO thin films was applied. According to this, the concentration of zinc acetate in the starting sol was maintained constant while the BAPPG oligomer was varied in a ratio BAPPG/Znacac = 0.5–5. Before we discuss the effect to the resulting ZnO film morphology varying the experimental parameters adding more quantity of BAPPG, the possible reaction mechanism should also be considered. In Fig. 1 the IR spectra of pure BAPPG, Znacac and their resulting mixture before and after heat treatment are presented. All data concern to thin films of the materials on silicon wafers prepared with dip-coating from *i*-prOH solutions. The presence of the two

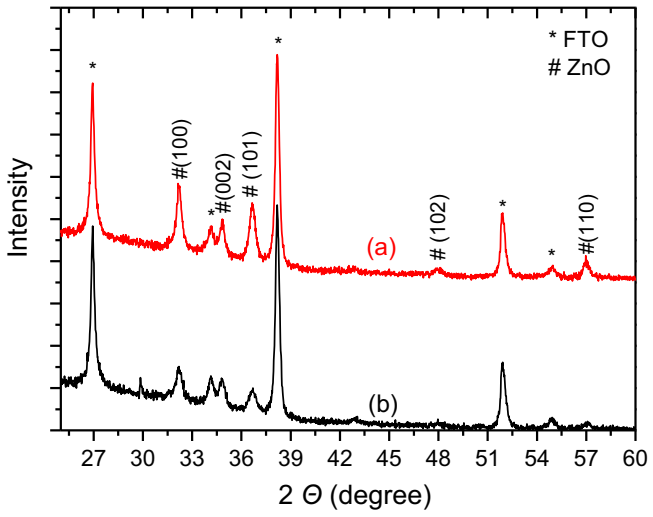

Fig. 2. XRD spectra of ZnO films on FTO glass for: (a) 0.5 and (b) 5, BAPPG/Znacac molar ratio.

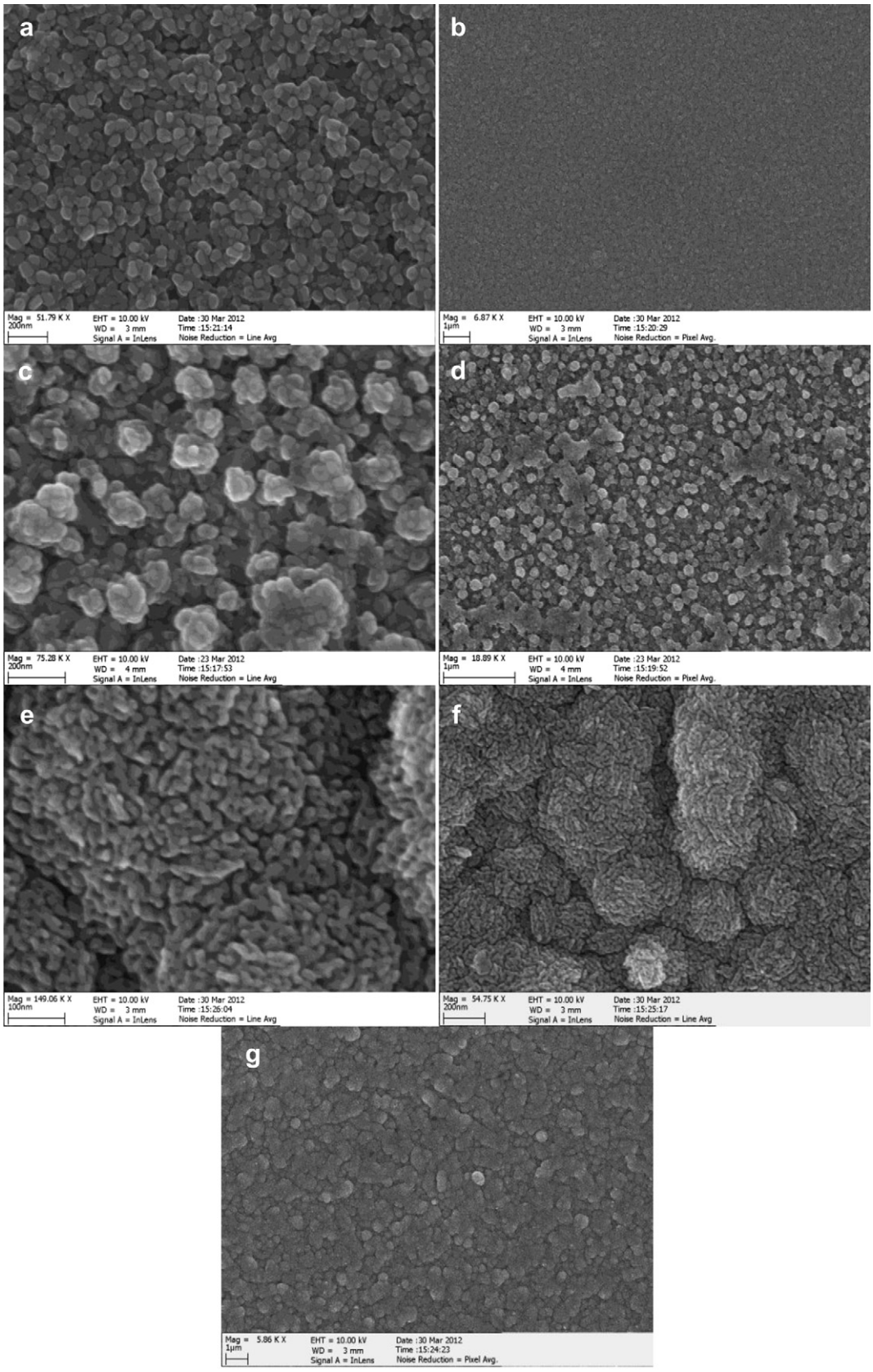

Fig. 3. SEM images of ZnO films made of BAPPG/Znacac = 0.5 (a,b), 2 (c,d), 5(e,f,g) molar ratio in low and high magnification.

stretching bands of primary amines at 3358 and 3290 cm^{-1} in BAPPG spectrum was seriously perturbed by the presence of Znacac. Two less intense peaks at 3248 and 3300 cm^{-1} are then appear. Besides, in the case of Znacac spectrum the band at 1440 cm^{-1} attributed to the asymmetric C=O stretching mode is slightly red-shifted by 20 cm^{-1} when the BAPPG was added to the sol. The above findings suggest that amine groups could behave like a nucleophile and attack electron-deficient carbon of carbonyl group of acetate [36]. Furthermore, as it can be also proved by the evidences of microscopy technique the amine groups in combination with oligomer chain could also behave as a template to the final formation of the ZnO nanostructure. A proposed mechanism for particle formation and the role of BAPPG is presented on Scheme 1. Finally, a clear evidence of Zn–O band at 415 cm^{-1} is observed after film heat treatment at 500 °C.

Fig. 2 shows the results of XRD spectra of the ZnO films prepared on FTO conductive glass using 0.5 and 5 BAPPG/Znacac molar ratios. Distinctive diffraction peaks at 2-theta angle of 31.8°, 34.5°, 36.2°, 47.6° and 56.6° are attributed to (100), (002), (101), (102) and (110) crystal planes of ZnO respectively. The relative intensity of ZnO crystal plane peaks at both cases in Fig. 2 is not the same so the use of more BAPPG quantity may favor the growth of (100) and (101) crystal planes. Grain size of ZnO particles of both films has been calculated from XRD patterns using Scherrer's equation: $D = 0.9\lambda/(s \cos \theta)$, where λ is the wavelength of the X-ray and s is the full width (radians) at half maximum (FWHM) of the signal. The calculation was performed for (100) crystal plane where the peak at XRD pattern was more intense. The calculated particle size was 33 nm for BAPPG/Znacac molar ratio = 0.5 while it was found 16.6 nm for molar ratio = 5 which were finally in accordance with SEM experimental results.

The morphology and the particle size of ZnO films are presented in Fig. 3. Typical SEM images correspond to the samples using 0.5, 2 and 5 BAPPG/Znacac molar ratios. In all cases the films exhibit smooth surface with no crack formation. The good mechanical stability of the films on FTO conductive glass is generally due to the chemical bonds (i.e., Zn–O–Sn) induced by the high calcination temperature (i.e., 500 °C). It is obvious that in the case of low BAPPG content (0.5 BAPPG/Znacac molar ratio) the films are consisted of uniform ZnO nanoparticles with average particle size 25–30 nm and very low degree of aggregation. Increasing the quantity of the BAPPG (BAPPG/Znacac molar ratio equivalent to 2) the particles appear to be in aggregated form in a rather spherical shape and average diameter around to 100 nm. Each ZnO aggregate consisted of nanosized crystallites of ~30 nm. In the magnified image (Fig. 3d) the films seem to be homogeneous with no cracks consisted of monodisperse aggregates of ZnO particles. When the BAPPG/Znacac molar ratio was further increased (equal to 5) then different film morphology was observed which is presented in Fig. 3e–g. Big sphere shape aggregates of average diameter 200–350 nm appeared (Fig. 3f) while these spheres are consisted of small particles with elongated shape and average size of 10 nm (Fig. 3e). The film is still homogeneous with no cracks that is very important for the construction of efficient solar cells (Fig. 3g).

QD sensitized wide band gap semiconductors is a promising prospect to the solar cell technology with significant potential in recent years while CdS and CdSe QD-sensitizers are reported to exhibit better performance among other QDs. Therefore, the as-prepared ZnO films, either consisted of monodispersed or aggregated particles, were covered with CdS and CdSe quantum dots using SILAR and CBD method respectively. The 2.25 eV energy band gap of CdS is a major drawback to the construction of an efficient solar cell as it limits the absorption of the sensitized films in the visible. However the co-presence of CdSe could extend the absorption in the visible and near IR region of solar light. The CdS

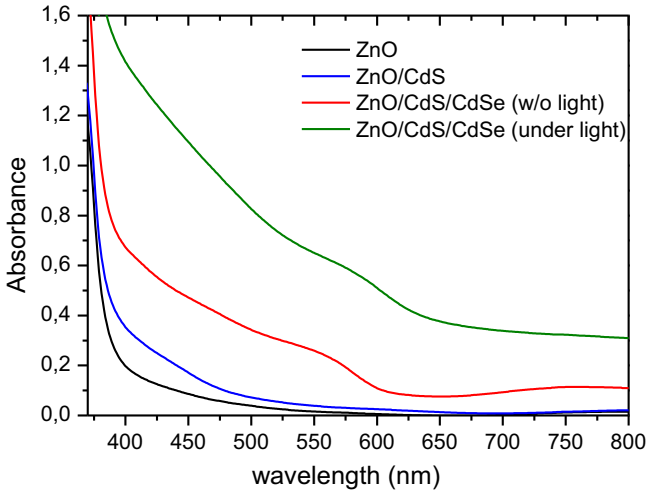

Fig. 4. Absorbance of bare or CdS sensitized and CdSe/CdS co-sensitized ZnO films.

quantity on ZnO films was controlled by successive dipping in Cd^{2+} and S^{2-} aqueous solutions as described in the experimental section (SILAR). Besides, for the co-sensitization of the ZnO films with CdSe these were stayed in a $Na_2SeSO_3/Cd(NO_3)_2$ mixture in water while the CdSe quantity was controlled with time and artificial light illumination of the samples. Fig. 4 shows the absorption of pure ZnO films and sensitized with CdS or CdS/CdSe QDs. It is obvious that the presence of CdSe causes an enhanced absorption of the films in the visible and near IR. In addition, the CdSe QDs growth on ZnO was affected by the ambient light. In particular, when the ZnO films in QDs sol were exposed to artificial solar light an increase to the CdSe deposition rate was noticed.

The influence of the as-prepared ZnO thin films with different structural properties on the QDSSC performance was finally examined. The solar cell performance was characterized measuring the current density–voltage curves of samples with monodispersed or aggregated ZnO nanoparticles where the BAPPG/Znacac molar ratio was 0.5 and 5 respectively. Considering the fact that film thickness is an important factor to affect photovoltaic behavior of the cells, the film thickness of two types of films was also investigated using cross-section SEM technique. A comparable

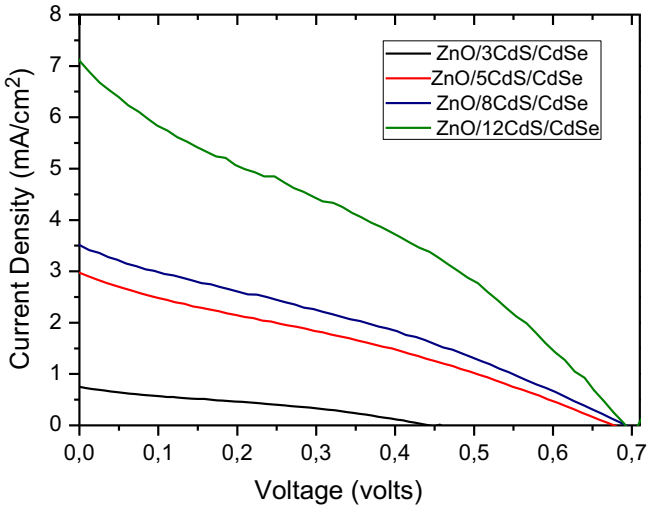

Fig. 5. *J–V* curves at simulated AM 1.5, 1 sun Xe-light for the QDSSCs constructed with ZnO films consisted of monodispersed particles and variable cycles of CdS deposition.

Table 1
Solar cell parameters from *J–V* curves of CdS/CdSe co-sensitized monodispersed particle ZnO electrodes.

Electrode ZnO/CdS/CdSe/ZnS (CdS cycles)	J_{SC} (mA cm^{-2})	V_{OC} (volts)	*ff*	*n* (%)
3	0.75	0.44	0.31	0.1
5	3.0	0.67	0.30	0.6
8	3.5	0.69	0.31	0.75
12	7.1	0.69	0.31	1.5

Table 2
Solar cell parameters from *J–V* curves of CdS/CdSe co-sensitized aggregated particle ZnO electrodes.

Electrode ZnO/CdS/CdSe/ZnS (CdS cycles)	J_{SC} (mA cm^{-2})	V_{OC} (volts)	*ff*	*n* (%)
3	1.2	0.58	0.40	0.28
5	7.1	0.73	0.40	1.9
8	8.6	0.71	0.41	2.5
12	16.3	0.68	0.41	4.5

film thickness of the two types of films was observed and it was found to be around 500 nm. The CdSe was formed as a thin film over ZnO consisted of very small quantum sized particles with an average size of 3–5 nm.

The QDSSC performance for ZnO monodispersed particles as a function of CdS quantity is presented on Fig. 5. Results are presented in Table 1 where a maximum 1.5% overall performance was monitored in case of twelve successive coating cycles of CdS. It is worth to mention that in case of three coating cycles the performance of the cells are poor as the quality of the resulting composite film (ZnO/CdS/CdSe) after washing out the residual material is also poor. The addition of more CdS quantity improves the stability of the films after CdSe deposition which affects also to the electrical performance of the cells.

The QDSSC performance for ZnO aggregated particles as a function of CdS quantity is also presented on Fig. 6. The efficiencies of the cells are comparative higher to those obtained for similar measurements of ZnO films with monodispersed particles (cf. Table 2). Indeed the maximum performance was measured 4.5% for twelve successive coating cycles of CdS. However, the efficiency of 4.5% can be considered among the highest are monitored for QDSSC employing ZnO films [37]. The better performance obtained for ZnO aggregated particles is due to the significant difference in the short-circuit current density and fill factor values resulting in a difference to the overall conversion efficiency. We believe that light scattering and photon localization within the film consisting of submicrometer sized aggregates could be happen which are favorable to achieve a solar cell with higher performance [38].

The ZnO film was consisted of six successive layers of the material as it proved to be the optimum thickness in accordance to the efficiency of the cells (∼500 nm). Indeed we concluded to the optimum ZnO thickness after we examined the efficiency of the cells employing ZnO films with different number of deposition layers. In Fig. 7 we present the results, where it is obvious that after six successive layers the efficiency of the cells was decreased. In all experiments twelve cycles of CdS were used as it was proved to be the optimum quantity.

The presence of CdS between ZnO and CdSe enhances the performance of the solar cells therefore we may correlate it with the advantageous collection of the excited electrons from CdSe to ZnO [39]. Furthermore, the growth of CdSe QDs on ZnO is favored in the presence of CdS while in its absence the growth of CdSe takes more time.

At all above samples a thin layer of ZnS was deposited on CdSe QDs with successive dipping of the film in Zinc acetate and Sodium sulfide aqueous solutions respectively. The advantage of ZnS coating is the passivation of the surface states of CdSe which results in the suppression of the surface trapping of photoexcited electrons and holes in the CdSe QDs [40]. So the presence of ZnS layer inhibits the recombination of excited electrons at the CdSe/electrolyte interface and protects the QDs from photocorrosion. Extending our experiments by increasing the cycles of ZnS deposition on CdSe QDs we found that there was a decrease to the efficiency of our cells. In particular, when three cycles of ZnS were used we monitored a 7.5% decrease in the photocurrent and 9% decrease in the photovoltage of the cells. Furthermore, we tried to interpose a layer of ZnS directly on ZnO before we apply SILAR method for CdS deposition. The results can be directly compared with those obtained for ZnO films without the presence of ZnS. Therefore we may conclude that the presence of ZnS is quite necessary after deposition of CdSe QDs and also one cycle of deposition is enough to obtain a protective shell to the CdSe.

It is noteworthy that the above described efficiencies for ZnO QDSSC cells were obtained with quasi-solid electrolyte, employing

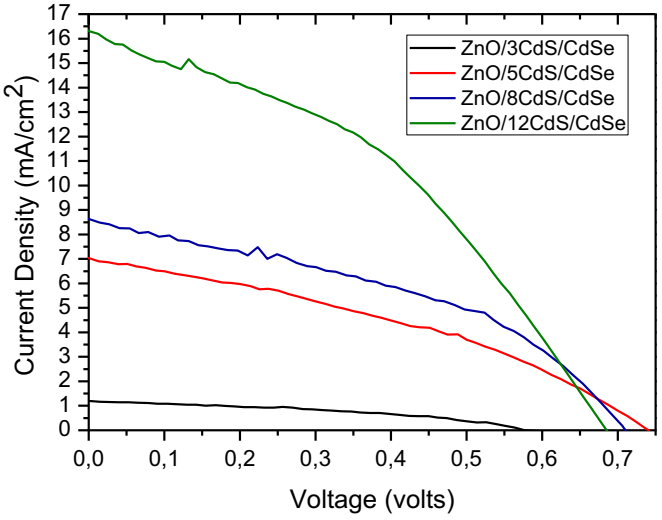

Fig. 6. *J–V* curves at simulated AM 1.5, 1 sun Xe-light for the QDSSCs constructed with ZnO films consisted of aggregated particles and variable cycles of CdS deposition.

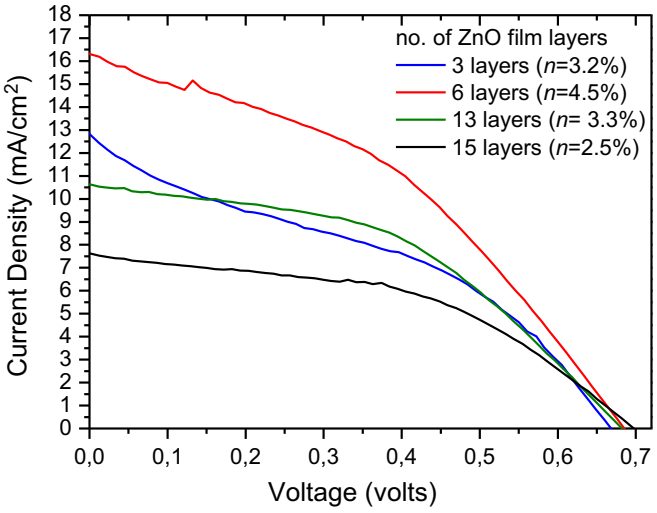

Fig. 7. *J–V* curves at simulated AM 1.5, 1 sun Xe-light for the QDSSCs constructed with ZnO films consisted of aggregated particles and different film thickness.

Table 3
Solar cell parameters from *J*–*V* curves of CdS/CdSe co-sensitized aggregated particle ZnO electrodes with aqueous and quasi-solid state electrolyte.

Electrode ZnO/CdS/CdSe/ZnS	J_{SC} (mA cm^{-2})	V_{OC} (volts)	*ff*	*n* (%)
6layers/12cycles/1day/1c/ aqueous electrolyte	7.6	0.53	0.30	1.2
6layers/12cycles/1day/1c/ Quasi-solid electrolyte	16.3	0.68	0.41	4.5

polysulfide (S^{2-}/S_x^{2-}) redox electrolyte. We used methanol as main solvent for the preparation of quasi-solid electrolyte where the solubility of sulfur is better compared to water. The efficiency of the cells with water free organic–inorganic composite host material was doubtless higher whilst it was poor using pure water [41]. According to data of Table 3 there was a 73% decrease to the overall efficiency of the cells when the quasi-solid electrolyte was substituted with an aqueous electrolyte with the same quantity (S^{2-}/S_x^{2-}) redox couple. Therefore, in common water based electrolytic solution, poor solubility induces a low dissolved amount of polysulfide redox relay, and for Pt based counter electrode depletion of the redox relay can occur due to adsorption of sulfur compounds on the electrode surface.

4. Conclusions

This study presents a new method for the preparation of ZnO nanocrystalline films for the fabrication of electrodes in quantum dots solar cells. Transparent films consisted of monodispersed or aggregated particles of ZnO depending on the quantity of BAPPG oligomer can be easily formed on FTO conductive glass via a dip coating technique. QDSSCs with co-sensitized ZnO films with CdS and CdSe were constructed while a quasi-solid electrolyte was employed for first time. The constructed solar cells showed high solar to electrical energy conversion efficiency (4.5%) under 1 sun and 1.5 AM light irradiance. The use of ZnO films with aggregated particles proved to be more efficient to the conversion of solar light while the quasi-solid electrolyte was more advantageous to the usually employed aqueous electrolytes.

Acknowledgments

Prof. E. Stathatos would like to acknowledge the financial support from “Archimedes III” co-funded by the European Union–European Social Fund and National Resources (NSRF 2007–2013). The authors would also like to thank Dr. Vassilios Dracopoulos, FORTH/ICE-HT, for the FE-SEM images.

References

[1] Y. Diamant, S. Chappel, S.G. Chen, O. Melamed, A. Zaban, Coord. Chem. Rev. 248 (2004) 1271–1276.
[2] R. Argazzi, N. Yukie, M. Iha, H. Zabri, F. Odobel, C.A. Bignozzi, Coord. Chem. Rev. 248 (2004) 1299–1316.
[3] M. Gratzel, Curr. Opin. Colloid Interface Sci. 4 (1999) 314–321.
[4] B. O'Regan, M. Grätzel, Nature 353 (1991) 737–740.
[5] J.B. Baxter, J. Vac. Sci. Technol. A 30 (2) (2012). art. no. 020801.
[6] A. Yella, H.-W. Lee, H.N. Tsao, C. Yi, A.K. Chandiran, Md.K. Nazeeruddin, E.W.-G. Diau, C.-Y. Yeh, S.M. Zakeeruddin, M. Grätzel, Science 4 (2011) 629–634.
[7] A.B. Djurišić, X. Chen, Y.H. Leung, A.M. Ching Ng, J. Mater. Chem. 22 (2012) 6526–6535.
[8] V. Dhas, S. Muduli, W. Lee, S.H. Han, S. Ogale, Appl. Phys. Lett. 93 (2008) 243108–243110.
[9] Q. Zhang, C.S. Dandeneau, X. Zhou, G. Cao, Adv. Mater. 21 (2009) 4087–4108.
[10] J. Preat, D. Jacquemin, E.A. Perpète, Energy Environ. Sci. 3 (2010) 891–904.
[11] A. Mishra, M.K.R. Fischer, P. Bauerle, Angew. Chem. Int. Ed. 48 (2009) 2474–2499.
[12] Z. Lu, J. Xu, X. Xie, H. Wang, C. wang, S.-Y. Kwok, T. Wong, H.L. Kwong, I. Bello, C.-S. Lee, S.-T. Lee, W. Zhang, J. Phys. Chem. C 116 (2012) 2656–2661.
[13] H. Yang, W. Fan, A. Vaneski, A.S. Susha, W.Y. Teoh, A.L. Rogach, Adv. Funct. Mater. http://dx.doi.org/10.1002/adfm.201103074.
[14] H. Lee, M. Wang, P. Chen, D.R. Gamelin, S.M. Zakeeruddin, M. Gratzel, Md.K. Nazeeruddin, Nano Lett. 9 (2009) 4221–4227.
[15] K.S. Leschkies, R. Divakar, J. Basu, E. Enache-Pommer, J.E. Boercher, C.B. Carter, U.R. Kortshagen, D.J. Norris, E.S. Aydil, Nano Lett. 7 (2007) 1793–1798.
[16] H. Jin, S. Choi, R. Velu, S. Kim, H.J. Lee, Langmuir 28 (2012) 5417–5426.
[17] I. Barcelo, T. Lana-Villarreal, R. Gomez, J. Photochem. Photobiol. A: Chem. 220 (2011) 47–53.
[18] Q. Shen, A. Yamada, S. Tamura, T. Toyoda, Appl. Phys. Lett. 97 (2010) 123107.
[19] C. Wang, Z. Jiang, L. Wei, Y. Chen, J. Jiao, M. Eastman, H. Liu, Nano Energy 1 (2012) 440–447.
[20] M. Samadpour, A. Iraji zad, N. Taghavinia, M. Molaei, J. Phys. D: Appl. Phys. 44 (2011) 045103.
[21] S.M. Willis, C. Cheng, H.E. Assender, A.A.R. Watt, Nano Lett. 12 (2012) 1522–1526.
[22] J.J. Choi, Y.-F. Lim, M.B. Santiago-Berrios, M. Oh, B.-R. Hyun, L. Sun, A.C. Bartnik, A. Goedhart, G.G. Malliaras, H.D. Abruna, F.W. Wise, T. Hanrath, Nano Lett. 9 (2009) 3749–3755.
[23] S. Cheng, W. Fu, H. Yang, L. Zhang, J. Ma, H. Zhao, M. Sun, L. Yang, J. Phys. Chem. C 116 (2012) 2615–2621.
[24] P.P. Boix, G. Larramona, A. Jacob, B. Delatouche, I. Mora-Sero, J. Bisquert, J. Phys. Chem. C 116 (2012) 1579–1587.
[25] N. Guijarro, T. Lana-Villareal, Q. Shen, T. Toyoda, R. Gomez, J. Phys. Chem. C 114 (2010) 21928–21937.
[26] S. Gimenez, I. Mora-Sero, L. Macor, N. Guijarro, T. Lana-Villareal, R. Gomez, L.J. Diguna, Q. Shen, T. Toyoda, J. Bisquert, Nanotechnology 20 (2009) 295204.
[27] H.J. Lee, D.-Y. Kim, J.-S. Yoo, J. Bang, S. Kim, S.-M. Park, Bull. Korean Chem. Soc. 28 (2007) 953–958.
[28] I. Barcelo, J.M. Campina, T. Lana-Villarreal, R. Gomez, Phys. Chem. Chem. Phys. 14 (2012) 5801–5807.
[29] B. Sun, Y. Hao, F. Guo, Y. Cao, Y. Zhang, Y. Li, D. Xu, J. Phys. Chem. C 116 (2011) 1395–1400.
[30] F. Zhao, G. Tang, J. Zhang, Y. Lin, Electrochim. Acta 62 (2012) 396–401.
[31] L. Liu, Y. Chen, T. Gua, Y. Zhu, Y. Su, C. Jia, M. Wei, Y. Cheng, Appl. Mater. Interfaces 4 (2012) 17–23.
[32] E. Stathatos, P. Lianos, Adv. Mater. 19 (2007) 3338–3341.
[33] E. Stathatos, Y. Chen, D.D. Dionysiou, Sol. Energy Mater. Sol. Cells 92 (2008) 1358–1365.
[34] M. Fakis, E. Stathatos, G. Tsigaridas, V. Giannetas, P. Persephonis, J. Phys. Chem. C 115 (2011) 13429–13437.
[35] M. El Harakeh, L. Alawieh, S. Saouma, L.I. Halaoui, Phys. Chem. Chem. Phys. 11 (2009) 5962–5973.
[36] Z. Zhang, M. Lu, H. Xu, W.-S. Chin, Chem. Eur. J. 13 (2007) 632–638.
[37] Y.-L. Lee, Y.-S. Lo, Adv. Funct. Mater. 19 (2009) 604–609.
[38] Q. Zhang, T.P. Chou, B. Russo, S.A. Jenekhe, G. Cao, Adv. Funct. Mater. 18 (2008) 1654–1660.
[39] Y. Zhang, J. Zhu, X. Yu, J. Wei, L. Hu, S. Dai, Sol. Energy 86 (2012) 964–971.
[40] Q. Shen, J. Kobayashi, L.J. Diguna, T. Toyoda, J. Appl. Phys. 103 (2008) 084304.
[41] M. Seol, E. Ramasamy, J. Lee, K. Yong, J. Phys. Chem. C 115 (2011) 22018–22024.